Plant Physiol. (1992) 98, 279-286
0032-0889/92/98/0279/08/$01.00

Received for publication February 26, 1991
Accepted July 24, 1991

# Flow Cytometric Analysis of Rhodamine 123 Fluorescence during Modulation of the Membrane Potential in Plant Mitochondria

**Patrice X. Petit**

*Centre National de la Recherche Scientifique, (UPR39) Biochimie Fonctionnelle des Systèmes Membranaires Végétaux, groupe des Biosystèmes Membranaires, Batiment 24 and Service de Cytométrie (LP40), Gif sur Yvette, France*

## ABSTRACT

**The fluorescent dye rhodamine 123, which selectively accumulates in mitochondria based on the membrane potential, was used with flow cytometry to evaluate variations in activity of mitochondria isolated from plant tissues. In the presence of succinate and ATP, potato (*Solanum tuberosum* L.) tuber mitochondrial activity was affected by metabolic inhibitors and compounds that modify the membrane potential. The more uniform the mitochondrial population, the higher the observed membrane potential. The reactive population corresponds to the proportion of intact mitochondria (94–97%) defined by classic methods. Changes in the light-scattering properties are more related to internal modifications affecting the inner membrane-matrix system of the mitochondria during metabolic modulation than to specific volume change or outer membrane surface modifications. We tested our approach using an *Arum maculatum* preparation that contains three different types of mitochondria and demonstrated the validity of the light-scatter measurements to distinguish the α, β, and γ mitochondria and to measure their ability to built up a membrane potential in the presence of succinate. These results demonstrate clearly that flow cytometric techniques using rhodamine 123 can be employed to study the activity in isolated plant mitochondria.**

Fluorescent probes have been applied as optical indicators of the membrane potential differences in several types of cells, isolated organelles, and lipid vesicles (1, 4, 20, 31). The technique relies on membrane potential-dependent partitioning of charged lipophilic dye molecules across the membrane. Changes in membrane potential result in changes in the intensity of dye fluorescence, termed "redistribution signals" (4). Lipophilic cationic dyes have been used successfully to measure changes in the membrane potential of *in situ* or isolated mitochondria of yeast cells (9, 20), several kinds of animal cells (27), and, more recently, plant cells and protoplasts (13, 15, 26). In plant mitochondria, the dyes most widely used for mitochondria are either derivatives of rhodamine or cyanine dyes developed by Waggoner (30, 31). The laser dye, Rh123,[1] has been extensively employed as a fluorescent stain of mitochondria in living cells (27). Because Rh123 is an aromatic cation, it has been assumed to distribute itself electrophoretically into the mitochondrial matrix in response to $\Delta\Psi$.

At high concentrations, Rh123 has toxic side effects, but Emaus *et al.* (6) have recently demonstrated that, at concentrations that do not inhibit mitochondrial function, Rh123 is indeed a sensitive and specific probe of $\Delta\Psi$ in isolated mitochondria. Agents known to depolarize or deenergize mitochondria, such as uncouplers (valinomycin) and respiratory inhibitors (KCN, SHAM), decreased Rh123 fluorescence of mitochondria in cultured cells, whereas nigericin, which collapses $\Delta$pH and raises $\Delta\Psi$, increases fluorescence. For Rh123, the energy-linked changes were accompanied by dye uptake into the matrix space and the concentration ratio in-to-out reached 4000:1 (6). In rat liver mitochondria, Rh123 also inhibits ADP-stimulated respiration (state 3) with a $K_i$ of 12 $\mu$M and ATPase activity of inverted inner membrane vesicles with a $K_i$ of 126 $\mu$M (6, 14, 16).

Mitochondria are known to swell or shrink in response to changes in conditions of incubation. The volume changes are commonly followed by observing either the intensity of light scattered at 90° to the incident beam, or the absorbance of a suspension, the assumption being that as mitochondria swell, their relative refractive index decreases and so does the intensity of light they scatter. Measurements of the light scatter (7, 10) demonstrate that changes in the intensity of scattered light are not reliable indices of changes of volume of mitochondria, and that changes in conformation with changes in metabolic state dominate changes in light scatter. At present, we do not know if the flow cytometric analysis that considered uniquely the objects passing through the laser beam has provided similar information.

Flow cytometry measurements of individual organelles have been performed on purified mouse and rat liver mito-

[1] Abbreviations: Rh123, rhodamine 123; HCV, coefficient of variation calculated on the full width at half maximum of the integral of fluorescence; IGF, integral of green fluorescence; IGFL, logarithm of the integral of fluorescence, three-order scale; LP, long pass filter; $\Delta\Psi$, transmembrane potential difference; SP, short pass filter; $TPP^+$, tetraphenylphosphonium, FALS, forward low angle light scatter; r.u., relative units.

chondria (12, 19, 21, 24) and on mitochondria from plant tissues (17, 22). In the present report, we describe the use of the membrane potential-sensitive probe Rh123 to study the membrane potential-related fluorescence and the light scatter of purified plant mitochondria during modulation of the membrane potential.

## MATERIALS AND METHODS

### Preparation of Mitochondria

Potato (*Solanum tuberosum* L. cv Bintje) tuber mitochondria were prepared and purified on a Percoll step gradient as described by Petit *et al.* (23), with the modifications introduced by Sommarin *et al.* (29). Purified mitochondria were collected at the 23/40% Percoll interface and washed in 0.3 M mannitol, 0.1% BSA (fraction V, Sigma), and 10 mM Mops-KOH (pH 7.2) to remove the Percoll.

*Arum maculatum* mitochondria were isolated from the sterile part of the spadix on a discontinuous sucrose density gradient as described by Lance and Chauveau (11). The flow cytometry experiments were performed on the main mitochondrial population for each stage of spadix development, Mp3 for the $\alpha$ stage, Mp2 mitochondria for the $\beta$ stage, and Mp1 mitochondria for the $\gamma$ stage, according to Chauveau and Tuquet (3). The crude mitochondrial preparation is loaded at the top of a step sucrose gradient (11) and as the main bands are taken up from the gradient they are respectively named from the top of the gradient to the bottom, Mp1, Mp2, and Mp3.

### Flow Cytometry Analysis

Purified mitochondria (10–40 $\mu$g protein in 2 mL) were analyzed after staining with 5 nM rhodamine 123 (Eastman Kodak) on an EPICS V (Coulter Electronics, Hialeath, FL), with confocal optics and an argon laser (Spectra-Physics 2025-05, Mountain View, CA). The laser excitation was 488 nm and 400 mW. The filters used were 515 nm LP interference, 515 nm LP absorbance, and 560 SP interference. Mitochondrial autofluorescence tested in the absence of dye under different metabolic conditions (*i.e.* ± succinate, ± ADP, ± valinomycin) was found to vary less than 5%.

A standard 76 $\mu$m nozzle was used; we found that reducing the nozzle size did not improve the resolution. The sheath was water at room temperature at 89.6 kPa and a differential pressure of 48.3 to 89.6 kPa. Each analysis was performed on $10^5$ particles at a rate of 3 to $4 \cdot 10^3$ particles/s. Monoparametric representations were on 256 channels and biparametric representations were on a 64-channel scale.

For fluorescence measurement expression, we used IGFL, for which an increment of 27 channels (on 256 channels) represents a doubling. The dispersion of the mitochondrial population around the higher frequency peak was expressed as HCV, which was calculated from the full width at half maximum height on a linear scale (IGF). When a bimodal state is observed, a gating procedure allows the exact determination of the HCV for the pic of interest. IGFL was calculated from the values of the mean fluorescence channel $x$ (logarithmic scale) converted to linear scale with $y = 10$ exp $(1.1149\ 10^{-2} \cdot x)$ and normalized the sample with the highest fluorescence (succinate + ATP) as a reference within each experimental series.

### Metabolic Activity and Membrane Potential

Membrane potential was measured with a $TTP^+$ electrode (8) in parallel with oxygen uptake measurements at 25°C in an air-saturated medium. The value of the membrane potential was not corrected for the passive binding of the $TPP^+$ (28). The final volume of 3 mL contained 0.3 M mannitol, 10 mM KCl, 5 mM $MgCl_2$, 0.5 mg mL$^{-1}$ BSA, and 10 mM potassium phosphate (pH 7.2). The integrity of the outer mitochondrial membrane was estimated by the latency of Cyt *c* oxidase activity as described in ref. 17.

### Determination of Protein

Protein concentration was determined essentially as described (2) after solubilizing the samples in 5% (w/v) deoxycholate. BSA was used as the standard.

## RESULTS AND DISCUSSION

### Characteristics of the Mitochondrial Suspensions

Purified mitochondria exhibited a high degree of outer membrane integrity, with an average of 94 to 97% remaining intact. Respiratory activity in the presence of succinate and ADP was 240 ± 25 nmol $O_2$ min$^{-1}$ mg$^{-1}$ protein, with a respiratory control of 4.3 ± 0.3 ($n = 8$). A −220 to −230 mV membrane potential was generated under such conditions.

### Mitochondrial Membrane Potential and Flow Cytometry Analysis

Our goal was to determine if the flow cytometer could detect variations in membrane potential related to variations in mitochondrial metabolic activity (8) that may be associated with conformational changes affecting the inner mitochondrial membrane. Figure 1 shows a typical trace of the simultaneous measurement of $O_2$ consumption and of $\Delta\Psi$ in purified potato tuber mitochondria. The membrane potential-related fluorescence of Rh123 in cytometry is also presented according to the states marked along the trace.

After the calibration of the $TPP^+$ electrode with increasing $TPP^+$ concentration (2.5, 2.5, and 5 $\mu$M), a slight change was observed upon addition of mitochondria. This change is partly due to the dilution of the $TPP^+$ concentration by addition of the mitochondrial suspension, partly to an energy-independent uptake of $TPP^+$ by the mitochondrial population, and also to some background metabolic $\Delta\Psi$. The energy-independent uptake is probably due both to a nonspecific fixation of the cation (28) and to the presence of a Donnan potential in nonenergized mitochondria. The addition of respiratory substrate (succinate) stimulated an $O_2$ consumption and led to a decrease of the $TPP^+$ concentration in the medium, indicating a $TPP^+$ uptake by the mitochondria and the generation of a transmembrane potential of −220 to −230 mV (no net phosphorylation, state 4). The addition of ADP resulted in a concomitant increase in oxidation rate (state 3) and a release of the lipophilic cation from the mitochondria.

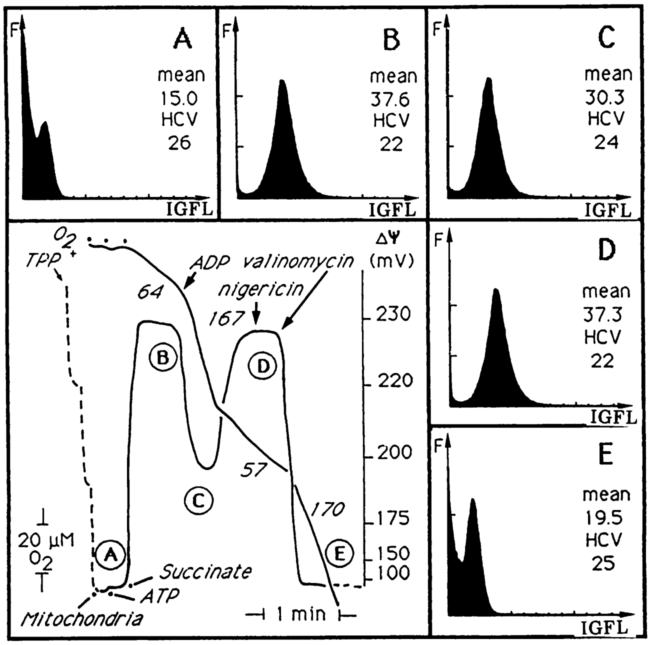


**Figure 1.** Simultaneous recording of oxidation rates and membrane potential of purified potato tuber mitochondria in parallel with flow cytometric analysis of the Rh123 membrane potential-related fluorescence. Where indicated, purified potato tuber mitochondria were added to a final concentration of 0.5 mg protein/mL. ATP (100 $\mu$M) was added before succinate (5 mM). A sufficient addition of ADP (200 $\mu$M) gave a steady-state three rate of $O_2$ uptake. The logarithmic span of the calculated (8) membrane potential is indicated, giving an idea of the limitation of the method; potentials below 100 mV are not measurable by this method. The rates of $O_2$ uptake are indicated on the polarographic trace. Nigericin was 100 ng mg$^{-1}$ protein and valinomycin 25 ng mg$^{-1}$ protein. The monoparametric histograms correspond to the marked points (A, B, C, D, and E): the $x$ axis is the fluorescence (IGFL) of the Rh123 on a 256 channel scale and the $y$ axis is the frequency. A, Mitochondria (20 $\mu$g ml$^{-1}$) + Rh123; B, mitochondria + Rh123 + succinate + ATP; C, transition in the presence of ADP; D, after ADP consumption and nigericin addition; and E, after addition of valinomycin and collapsing of the membrane potential. The mean fluorescent channels and the HCV (%), calculated on a linear scale (IGF), are indicated.

The value of the membrane potential in state 3 was about −195 mV. After phosphorylation occurred, the decrease in oxidation rate between states 3 and 4 was associated with an increase in membrane potential. The addition of nigericin, which converts any ΔpH into ΔΨ, did not modify the membrane potential, but the subsequent addition of valinomycin caused a collapse of the membrane potential.

Each stage of the membrane potential development could be correlated with the results obtained from the flow cytometry analysis of the membrane potential-related fluorescence of Rh123 (Fig. 1A–E). The autofluorescence of unstained mitochondria under these conditions was very low (result not shown). After addition of Rh123, the total fluorescence increased (Fig. 1A), but the mitochondria were not uniformly stained. In addition to a bright population, a second population exhibited a low intensity of fluorescence close to the autofluorescence level of the mitochondria. Moreover, the dispersion of the population was high (HCV 26), indicative of a heterogeneity of staining under nonenergized conditions. After addition of succinate (Fig. 1B), the fluorescence of the mitochondria increased. In addition, under these conditions, the histogram indicated a greater homogeneity of the mitochondrial population (HCV 22). The energized mitochondria, which are significantly more fluorescent than the nonenergized ones, represent approximately 94% of the mitochondrial population. Addition of ADP decreased the fluorescence (Fig. 1C), and, after full consumption of this limiting ADP, addition of nigericin did not increase the fluorescence (Fig. 1D). A subsequent addition of valinomycin (in the presence of $K^+$) to the energized mitochondria collapsed the membrane potential and lowered the fluorescence of individual organelles (Fig. 1E). However, the reduction of the fluorescence was not complete and the residual fluorescence remained higher than before energization. Furthermore, more mitochondria had significant fluorescence compared with nonenergized mitochondria (Fig. 1A). It seems that a small amount of dye that had access to internal binding sites during the energization of the mitochondria could not be removed during the deenergization.

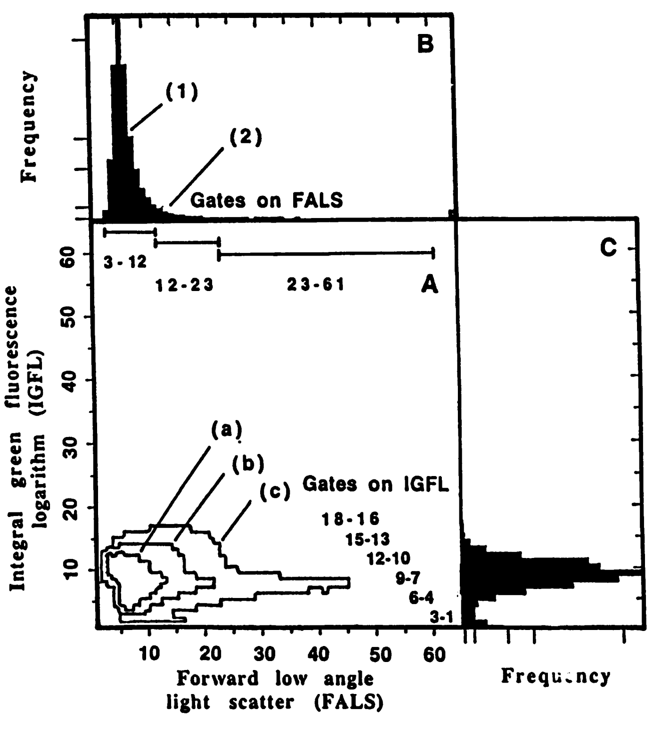


**Figure 2.** Cytogram corresponding to $10^5$ energized potato tuber mitochondria (succinate + ATP) comparing light scatter (FALS) and rhodamine 123 fluorescence (IGFL). A, Biparametric representation of FALS against IGFL. Three classes of frequency are indicated by the contours that delimit coordinates having (a) >250 mitochondria, (b) >50 mitochondria, and (c) >25 mitochondria. Corresponding histograms are shown as projections. B, Light scatter (FALS) and C, fluorescence (IGFL). In panel B, the numbers (1) and (2) distinguish, respectively, the mitochondrial subpopulation of low FALS (bell-shaped) and the mitochondrial subpopulation of high FALS.

### Membrane Potential and Light Scatter

Figure 2A shows the biparametric representation of the energized mitochondria (succinate + ATP) comparing observed FALS (Fig. 2B) and the Rh123 fluorescence (Fig. 2C). As can be seen, there is a bell-shaped population of low FALS values (a) and a minor population of higher FALS values (b). The "gating windows" were set as described in the legend to Figure 2A. These allow the study of one parameter as a function of the other.

Initially, gating windows on FALS signals are set to collect IGFL signals correlated with mitochondria displaying FALS signals in either the smaller (3–12 channels), the medium (12–24 channels), or the larger (24–61 channels) FALS subpopulations of purified mitochondria. As can be seen in Figure 3A, the mean fluorescence varied little as a function of the light scatter. The particles of medium and high light scatter (Fig. 3C and D) exhibit two subpopulations, one of lower and one of higher fluorescence than the population of lower light scatter (Fig. 3B). The proportion of mitochondria in the low and high fluorescence subpopulation changed as the light scatter changed.

The mitochondria of low FALS (Fig. 3B) are homogeneously distributed around the mean fluorescence value (mean IGFL = 8.0 ± 2.9), whereas the particles of high FALS belong to a widely distributed population containing both mitochondria of low fluorescent (mean IGFL = 6.6 ± 2.2) and of high fluorescent mitochondria (mean IGFL = 14.4 ± 3.7) (Fig. 3D). Contrary to expectation, the mitochondria of high FALS are composed of two subpopulations, one (the major) of low fluorescence and another (the minor) of high fluorescence.

Subsequently, we set gating windows on the IGFL (Fig. 4A). Analysis of the FALS values extracted from the gating windows designated on the fluorescence channels shows that 4% of the particles have high fluorescence, corresponding to particles having a high light scatter (FALS mean value 20.3) (Fig. 4B), and 96% of the particles having low or medium fluorescence belong to a low light scatter population with a mean FALS value of 8.0 (Fig. 4C). Thus, we conclude that there is a positive correlation between Rh123 staining and FALS; the higher the fluorescence, the higher the light scatter.

### Modulation of the Rhodamine 123 Fluorescence during NADH Oxidation

Table I describes the modulation of the mitochondrial membrane potential through successive additions of NADH, ADP and ionophores such as nigericin and valinomycin. To compare with the results obtained with the $TPP^+$ electrode (Fig. 1), the membrane potential values are presented.

The photomultiplier was set such that less than 1% of objects exceeded channel 20 fluorescence units. After addition of Rh123, the mean fluorescence increased, but the mitochondria were not uniformly stained (Fig. 1A). Few mitochondria exceed the initial arbitrary fluorescence threshold (6.7% > channel fluorescence 20).

After addition of NADH, the fluorescence of mitochondria increased as a consequence of the high membrane potential (−220 mV): 86% > channel 20. The distribution indicates more homogeneity (lower HCV) of the mitochondrial population with respect to the Rh123 fluorescence if compared with the nonenergized population (Table I). Addition of ADP decreased the membrane potential to −189 mV; accordingly, the IGFL decreased. Addition of nigericin in the presence of

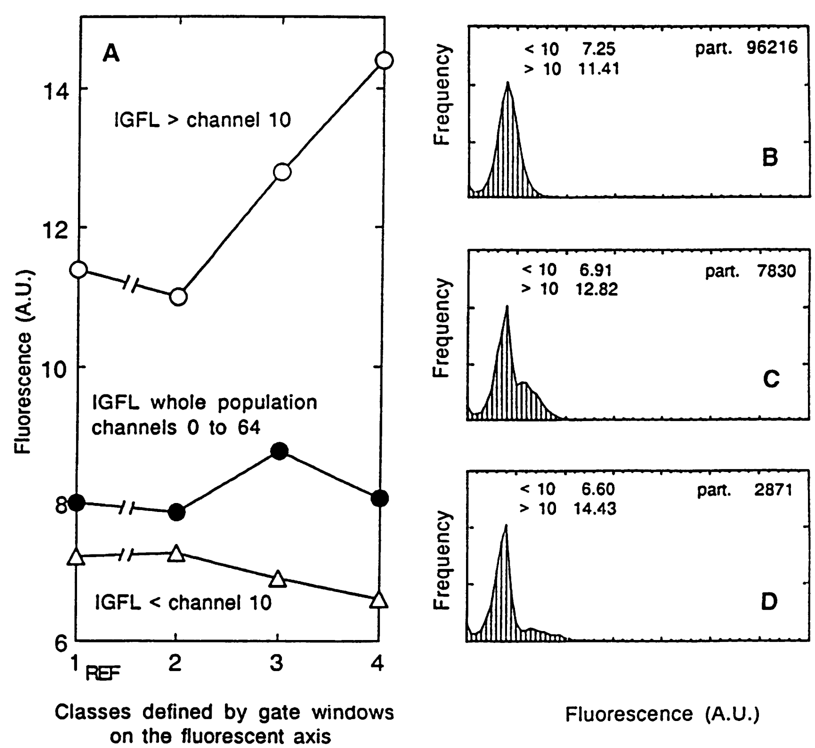


**Figure 3.** Analysis of rhodamine 123 fluorescence (IGFL) of energized potato tuber mitochondria (succinate + ATP) gated on the FALS. A, Fluorescence of the different classes of particles representing: 1, the whole mitochondrial population gated on FALS channels 3 to 61; 2, FALS channels 3 to 12; 3, FALS channels 12 to 23; 4, FALS channels 23 to 61. For a chosen gated population, the fluorescence mean value is given (●), as is the value of IGFL < channel 10 (△) or IGFL > channel 10 (○). The corresponding histograms are given in B for class 2, C for class 3, and D for class 4. Class 2 and class 1, representing the whole population, exhibit a similar pattern, and only the class 2 histogram is presented in B. The particles of channels 1 to 3 and 61 to 64 were discarded from the analysis to avoid, respectively, the measurement of low fluorescence of very small particles or "broken" mitochondria and the high fluorescence of the aggregated mitochondria. For B, C, and D, the number of mitochondria analyzed and the values of the gates are given.

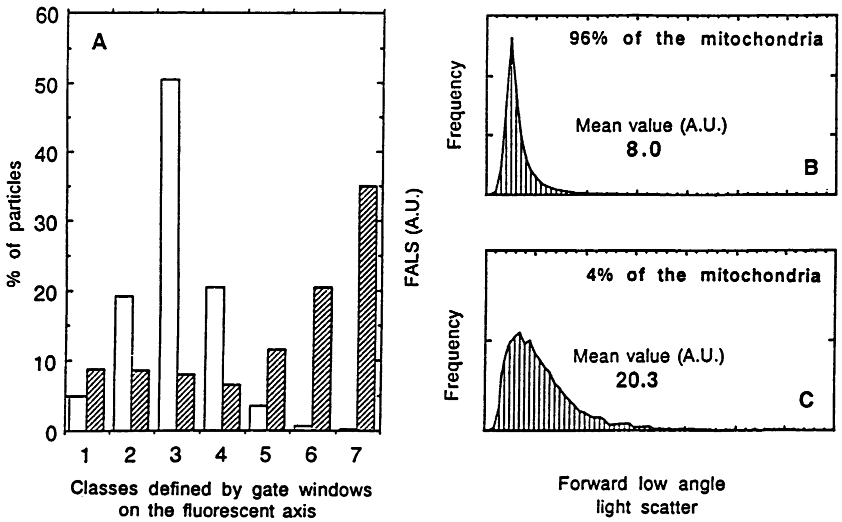


**Figure 4.** Analysis of the FALS of the energized mitochondria (succinate + ATP) gated on the rhodamine 123 fluorescence (IGFL). A, FALS of the different classes (1–7) of particles representing: the gates on IGFL, *i.e.* 1, channels 1 to 3; 2, channels 4 to 6; 3, channels 7 to 9; 4, channels 10 to 12; 5, channels 13 to 15; and 6, channels 16 to 18. The other channels contain no particles or less than 0.1% of particles and were not taken into account. B, Histogram FALS of classes 1 to 4, and (C) of classes 5 to 7. Non-hatched area, % of particles; hatched area, FALS.

$K^+$ did not modify $\Delta\Psi$ or IGFL. This result contrasts with that obtained with rat liver mitochondria studied under similar conditions (24) in which nigericin increased both $\Delta\Psi$ and fluorescence of Rh123, as expected from the conversion of the $\Delta pH$ into $\Delta\Psi$. However, it is in agreement with the succinate data discussed above. A subsequent addition of valinomycin to energized mitochondria lowered the fluorescence of individual organelles and increased heterogeneity (the HCV increased). However, as with succinate, the reduction of fluorescence was incomplete, with the residual fluorescence remaining higher than before energization (21% > channel fluorescence 20).

### Flow Cytometry Analysis in the Presence of Different Substrates

Table II shows the membrane potential-dependent fluorescence of mitochondria with different respiratory substrates. The values of the measured membrane potential under nonphosphorylating conditions varied slightly with the different substrates. For NADH and succinate, the $\Delta\Psi$ measured were close to −220 mV and decreased by about 33 to 35 mV under phosphorylating conditions. With malate (+ glutamate), the $\Delta\Psi$ was smaller (−186 mV) and the depolarization was less (31 mV).

The differences in Rh123 fluorescence measurated in the presence of different substrates was slightly larger than the difference in $\Delta\Psi$ recorded with the $TPP^+$ electrode, *i.e.* succinate 87.5, NADH 81, and malate (+ glutamate) 73.5 r.u.. The effect of ADP is also correlated to the decrease of the absolute values of the membrane potential and varied in a similar proportion.

Although the flow cytometric analysis of the Rh123 fluorescence changes are in agreement with the $TPP^+$ measurements of $\Delta\Psi$, it also provides an assessment of the uniformity

**Table I.** *Effects of ADP Addition on the Membrane Potential-Related Fluorescence of Rhodamine 123 in Potato Tuber Mitochondria Established in the Presence of NADH as Respiratory Substrate*

The photomultiplier setting was 1120 V and data were taken on $10^5$ particles; $\Delta\Psi$ was measured with a $TPP^+$ electrode as described in "Materials and Methods" and the reagents were 5 nM Rh123, 10 mM NADH, 100 $\mu$M ADP, 25 $\mu g\ mg^{-1}$ protein valinomycin, 0.1 $\mu g\ mg^{-1}$ protein nigericin, 20 $\mu g\ mL^{-1}$ protein purified potato mitochondria.

| Successive Additions | Respiration Rate[a] | Membrane Potential | IGFL (Mean Channel) | IGFL (Relative Values) | HCV[b] | Percent of Population over Channel 20 |
|---|---|---|---|---|---|---|
| | *nmol $O_2$ $min^{-1}$ $mg^{-1}$ protein* | *mV* | | | | |
| Mitochondria | | 0 | 1.3 | 41.5 | ND | <1 |
| + Rh123 | | 0 | 6.3 | 58.3 | 26 | 6.7 |
| + NADH | 45 | −220 | 27.3 | 100 | 22 | 85.9 |
| + ADP | 120 | −189 | 23.4 | 90.5 | 23 | 75.9 |
| + Nigericin | 119 | −220 | 27.4 | 100.3 | 22 | 86.3 |
| + Valinomycin | 173 | 0 | 12.5 | 66.5 | 25 | 21.5 |

[a] Respiratory activity measured within the oxygen electrode simultaneously with the membrane potential. [b] HCV calculated as described in "Materials and Methods," on a linear scale (IGF); when bimodal shape is observed, a gating procedure allows the exact determination of the HCV for the pie of interest.

**Table II.** *Membrane Potential-Related Fluorescence of Rhodamine 123 in Mitochondrial (Potato Tuber) Population Supplemented with Different Respiratory Substrates*

The photomultiplier setting was 1120 V and data were taken on $10^5$ particles; $\Delta\Psi$ was measured with a $TPP^+$ electrode as described in "Materials and Methods" and the reagents were 5 nM Rh123, 5 mM succinate, 10 mM NADH, 10 mM malate, 1 mM glutamate (as a starter), 100 $\mu$M ATP, 25 mg $mL^{-1}$ protein valinomycin, 0.1 $\mu$g $mg^{-1}$ protein nigericin, and 20 $\mu$g $mL^{-1}$ purified potato mitochondria.

| Successive Additions | Membrane Potential-Related Fluorescence (IGFL) | | Membrane Potential | Respiratory Activity |
|---|---|---|---|---|
| | Mean channel | Relative value | | |
| | | | *mV* | *nmol $O_2$ $min^{-1}$ $mg^{-1}$ protein* |
| Mitochondria | 1.3 | 41.5 | | |
| + Rh123 | 2.3 | 42.6 | | |
| + Succinate | 30.3 | 87.5 | −220 | 45 |
| + Succinate + ATP | 35.5 | 100 | −222 | 67 |
| + Succinate + ADP | 26.3 | 78.9 | −185 | 172 |
| + NADH | 27.3 | 81 | −220 | 43 |
| + NADH + ATP | 27.3 | 81 | −220 | 42 |
| + NADH + ADP | 23.4 | 73.3 | −187 | 122 |
| + Malate (+ glutamate) | 23.5 | 73.5 | −186 | 26 |
| + Malate (+ glutamate) + ATP | 23.6 | 73.7 | −187 | 27 |
| + Malate (+ glutamate) + ADP | 19.2 | 65.8 | −155 | 92 |

of conformational changes (FALS) taking place. Note that with the same $\Delta\Psi$, −220 mV, succinate gave an IGFL of 87.5 and NADH of 81 r.u.. Succinate oxidation is stimulated by ATP addition (27), but the membrane potential stays unchanged. However, the membrane potential-dependent fluorescence of Rh123 was enhanced, IGFL going from 87.5 to 100 r.u., and the mitochondrial population became more uniform (HCV decreased; data not shown). The addition of ADP in the presence of the three substrates induced a fluorescence decrease in parallel with the $\Delta\Psi$ decrease (Table II).

### Application of the Method with *Arum maculatum* Spadix Mitochondria

The $\alpha$, $\beta$, and $\gamma$ types of mitochondria differ in ultrastructure as described by Chauveau and Tuquet (3), but the volume delimited by the outer membrane appears unchanged. The FALS (Table III) also differ among the mitochondrial types: 62.3 for $\alpha$; 50.7 for $\beta$; and 42.7 r.u. for $\gamma$. This means that it is changes in the inner membrane and matrix that are affecting the light scatter properties of the mitochondria.

Three types of mitochondria exhibited a minor decrease in light scatter during the energization and an increase in light scatter increase during the deenergization (Table III). This means that flow cytometry analysis of the light scatter can discriminate inner membrane-matrix changes linked to metabolic variation through light scatter.

The $\alpha$, $\beta$, and $\gamma$ mitochondria differ in the maximal Rh123 fluorescence reached with succinate as a substrate, less for the $\alpha$ and $\beta$ types than for the $\gamma$ type: for IGFL, $\gamma$ = 100; $\beta$ = 92.7; $\alpha$ = 84.7 r.u. The effect of ATP on succinate oxidation is very important in $\alpha$ and $\beta$ types (increment of 10.8 and 9.9

**Table III.** *Rhodamine 123 Fluorescence and Forward Low Angle (10–20°) Light Scatter of $\alpha$, $\beta_1$ and $\gamma$ Types of Purified A. maculatum Mitochondria*

The photomultiplier setting was 1120 V and data were taken on $10^5$ particles; $\Delta\Psi$ was measured with a $TTP^+$ electrode as described in "Materials and Methods" and the reagents were 5 nM Rh123, 5 mM succinate, 100 $\mu$M ATP, 25 $\mu$g $mL^{-1}$ protein valinomycin, and 20 $\mu$g $mL^{-1}$ purified mitochondria. IGFL was calculated from the values of the mean fluorescence channel (logarithmic scale) converted to linear scale and to relative units.

| Conditions | Mitochondria Type $\alpha$ | | Mitochondria Type $\beta$ | | Mitochondria Type $\gamma$ | |
|---|---|---|---|---|---|---|
| | IGFL | FALS | IGFL | FALS | IGFL | FALS |
| Mitochondria | 61.9 | 62.3 | 61.8 | 50.6 | 60 | 42.7 |
| + Rhodamine 123 | 67.1 | | 72.6 | | 64.2 | |
| + Succinate | 73.9 | | 82.8 | | 97.3 | |
| + ATP | 84.7 | 60.9 | 92.7 | 50.1 | 100 | 39.4 |
| + Valinomycin | 72.5 | 62.8 | 73.2 | 54.0 | 75.1 | 49.2 |

r.u.) and very low with the $\gamma$ type (increment of 2.7 r.u.), whereas the absolute level of the fluorescence with succinate is close to the maximum (97.3 r.u.) without ATP.

## CONCLUSION

The flow cytometric analysis of the membrane potential-dependent fluorescence allows description of the mitochondrial population under different metabolic situations. Low probe concentration (5 nM Rh123) avoids the uncoupling effect of Rh123 (11–13), at much higher concentrations (8, 19). This low probe concentration is possible because of the optical advantages of the flow cytometer compared with conventional fluorometers.

The integrity (94–97%) of the Percoll-purified potato tubers mitochondria correlated with the percentage of particles able to built up a membrane potential in the presence of succinate and ATP (96% over channel 10, Fig. 1).

In studies of whole plant or animal cells, differences in light scattering properties are typically used to distinguish the size of the objects. However, as previously described (24), with particles less than 1 $\mu$m measured on a relatively large FALS (11–20°), the correlation between particle size and right angle light scatter no longer holds (16). The 11 to 20° used in this study is indeed wide, considering the small size of the potato tuber mitochondria (0.6 $\mu$m as mean value [22] determined by flow cytometry analysis and correlated with an the electron microscopic evaluation). In this situation, the FALS acquires some characteristics of broad (90°) angle light scattering in that it is sensitive to the internal state of the organelle and to the nature and state of the membrane components. The light scatter thus measures primarily the internal changes in the inner membrane and matrix of the mitochondria. Their is no simple relation between the "size" or the "volume" of the mitochondria and the FALS (24).

When deenergized mitochondria exhibited heterogeneous Rh123 staining, hyperpolarization reduced the dispersion of the population (low HCV), especially when the $\Delta\Psi$ was at its maximum (Fig. 1, Table I). In the resting state, the composition of the mitochondrial membranes plays a major role in the initial Rh123 binding. Other characteristics of purified mitochondria, *i.e.* surface charge density and Donnan potential, are additional factors of these intrinsic membrane determinants, *i.e.* lipid/protein ratio, degradation process to explain the initial dye binding or the residual dye fluorescence after deenergization. The high affinity binding sites for cationic lipophilic probes described by Colonna *et al.* (5) could be associated with the fact that the fluorescence does not go back to the initial level after deenergization. A similar heterogeneity has been noted for purified animal mitochondria (24) and plant mitochondria (22).

The use of the method we have devised to study the fluorescence and light scatter characteristics of different types of *A. maculatum* mitochondria has demonstrated the precision and applicability of flow cytometry analysis.

The advantages of flow cytometry over measurements upon bulk suspensions are multiple: (a) use of extremely small samples facilitating the study of mitochondria extracted from protoplasts, or from parts of the plant where the yield is low and not adequate for the $O_2$ or $TPP^+$ electrode measurements; (b) assessment of population uniformity; (c) multivariate analysis of attributes of individual mitochondria (19, 21, 24); (d) possibility of sorting subpopulations for subsequent analysis if micromethods are available.

## ACKNOWLEDGMENTS

The author would like to thank P. Müller and D. Marie for their technical assistance, and S.C. Brown, P. Diolez, and S. Sazer for helpful discussions.

## LITERATURE CITED

1. **Bashford CL** (1979) The use of optical probes to monitor membrane potential. Methods Enzymol **55:** 569–586
2. **Bradford MM** (1976) A rapid and sensitive method for the quantification of microgram quantities of protein using the principle of protein-dye binding. Anal Biochem **72:** 248–254
3. **Chauveau M, Tuquet C** (1985) Changes in structure and activities of *Arum maculatum* mitochondria during spadix development. Biol Cell **53:** 51–60
4. **Cohen LB, Salzberg BM** (1978) Optical measurement of membrane potential. Annu Rev Physiol Biochem Pharmacol **83:** 35–88
5. **Collona R, Massari S, Azzone GF** (1973) The problem of cationic binding sites in the energized membrane of intact mitochondria. Eur J Biochem **34:** 577–585
6. **Emaus KR, Grunwald R, Lemaster JL** (1986) Rhodamine 123 as a probe of transmembrane potential in isolated rat liver mitochondria: spectral and metabolic properties. Biochim Biophys Acta **850:** 436–448
7. **Garlid KD, Beavis AD** (1985) Swelling and contraction of the mitochondrial matrix. I. Quantitative application of the light scattering technique to solute transport across the inner membrane. J Biol Chem **260:** 13434–13441
8. **Kamo N, Muratsugu M, Hongoh R, Kobatake Y** (1979) Membrane potentiel of mitochondria measured with an electrode sensitive to tetraphenylphosphonium and relationship between proton electrochemical potential and phosphorylation potential in steady state. J Membr Biol **49:** 105–121
9. **Kovac L, Bohmerova E, Butko P** (1982) Ionophores and intacts cells I: valinomycin and nigericin act preferentially on mitochondria and not on the plasma membrane of *Saccharomyces cerevisiae*. Biochim Biophys Acta **721:** 341–348
10. **Knight VA, Wiggins PM, Harvey JD, O'Brien JA** (1981) The relationship between the size of mitochondria and the intensity of light that they scatter in different energetic states. Biochim Biophys Acta **637:** 146–151
11. **Lance C, Chauveau M** (1975) Evolution des activités oxydatives et phosphorylantes des mitochondries de l'Arum maculatum L. au cours du développement de l'inflorescence. Physiol Vég **13:** 83–94
12. **Lopez-Mediavilla C, Orfao A, Gonzalez M, Medina JM** (1989) Identification by flow cytometry of two distinct Rhodamine 123-stained mitochondrial population in rat liver. FEBS Lett **254:** 115–120
13. **Liu Z, Bushinell WR, Brambl RR** (1987) Potentiometric cyanine dyes are sensitive probes for mitochondria in intact plant cells. Plant Physiol **84:** 1385–1390
14. **Mai M, Allison WS** (1983) Inhibition of an oligomycin sensitive ATPase by cationic dyes, somes of which are atypical uncouplers of the intact mitochondria. Arch Biochem Biophys **221:** 467–476
15. **Matzke MA, Matzke JM** (1986) Visualization of mitochondria and nuclei in living plant cells by the use of a potential sensitive fluorescent dye. Plant Cell Environ **9:** 73–77
16. **Modica-Napolitano JS, Weiss MJ, Chen LB, Aprille JR** (1984) Rhodamine 123 inhibits bioenergetic function in isolated rat liver mitochondria. Biochem Biophys Res Commun **118:** 717–723
17. **Møller IM, Linden AC, Ericson I, Gardeström P** (1987) Isolation of submitochondrial particles with different polarities. Methods Enzymol **148:** 442–453

18. **Neuburger M, Journey EP, Bligny R, Carde JP, Douce R** (1982) Purification of plant mitochondria by isopycnic centrifugation in density gradients of Percoll. Arch Biochem Biophys **217**: 312–323
19. **O'Connor JE, Vargas JL, Kimler BF, Hernandez-Yago J, Grisolia S** (1988) Use of rhodamine 123 to investigate alterations in mitochondrial activity in isolated mouse liver mitochondria. Biochem Biophys Res Commun **151**: 568–573
20. **Pena A, Urbine S, Pardo JP, Borbolla M** (1984) The use of cyanine dye in measuring membrane potential in yeast. Arch Biochem Biophys **231**: 217–225
21. **Petit PX, Diolez P, de Kouchkovsky Y** (1990) Flow cytometry of energy transducing cellular organelles: mitochondria and chloroplasts. *In* A Yen, ed, Flow Cytometry: Advanced Research and Clinical Applications, Vol I. CRC Press, Boca Raton, FL, pp 271–303
22. **Petit P, Diolez P, Müller P, Brown SC** (1986) Binding of concanavalin A to the outer membrane of potato tuber mitochondria detected by flow cytometry. FEBS Lett **196**: 65–70
23. **Petit PX, Edman KA, Gardeström P, Ericson I** (1987) Somes properties of mitochondria, mitoplast and submitochondrial particles of different polarities from plant tissues. Biochim Biophys Acta **890**: 377–386
24. **Petit PX, O'Connor JE, Grunwald D, Brown SC** (1990) Analysis of membrane potential of rat and mouse liver mitochondria by flow cytometry and possible applications. Eur J Biochem **194**: 389–397
25. **Raison JK, Laties GG, Crompton U** (1973) The role of state 4 electron transport in the activation of state 3 respiration in potato mitochondria. J Bioenerg **4**: 409–422
26. **Reich TJ, Iver IV, Haffner M, Holbrook LA, Miki LB** (1986) The use of fluorescent dyes in the microinjection in alfalfa protoplastes. Can J Bot **64**: 1259–1267
27. **Ronot X, Benel L, Adolphe M, Mounolou JC** (1986) Mitochondrial analysis in living cells: the use of rhodamine 123 and flow cytometry. Biol Cell **57**: 1–8
28. **Rottenberg H** (1984) Membrane potential and surface potential in mitochondria: uptake and binding of lipophilic cations. J Membr Biol **81**: 127–138
29. **Sommarin M, Petit PX, Möller IM** (1990) Endogenous protein phosphorylation in purified plant mitochondria. Biochim Biophys Acta **1052**: 195–203
30. **Waggoner AS** (1976) Optical probes of membrane potential. J Membr Biol **27**: 317–334
31. **Waggoner AS** (1978) The use of cyanine dyes for the determination of membrane potential in cells, organelles, and vesicles. Methods Enzymol **55**: 689–695